


RESEARCH ARTICLE



Controlling the interaction between CaMKII and Calmodulin with a photocrosslinking unnatural amino acid

Iva Lučić^{1,2} | Pin-Lian Jiang² | Andreas Franz³ | Yuval Bursztyn¹ |
Fan Liu^{2,4} | Andrew J. R. Plested^{1,2,5} 

¹Institute of Biology, Cellular Biophysics, Humboldt Universität zu Berlin, Berlin, Germany

²Leibniz Forschungsinstitut für Molekulare Pharmakologie (FMP), Berlin, Germany

³Freie Universität Berlin, Institute of Chemistry and Biochemistry, Berlin, Germany

⁴Charité-Universitätsmedizin Berlin, Berlin, Germany

⁵NeuroCure, Charité Universitätsmedizin, Berlin, Germany

Correspondence

Andrew J. R. Plested and Iva Lučić, Institute of Biology, Cellular Biophysics, Humboldt Universität zu Berlin, Philippstr. 13, Berlin, Germany. Email: andrew.plested@hu-berlin.de and iva.lucic@hu-berlin.de

Funding information

Deutsche Forschungsgemeinschaft, Grant/Award Numbers: 278001972, 323514590, 446182550; European Research Council, Grant/Award Number: 949184; FP7 People: Marie-Curie Actions, Grant/Award Number: 798696

Review Editor: Aitziber L. Cortajarena

Abstract

Using unnatural amino acid mutagenesis, we made a mutant of CaMKII that forms a covalent linkage to Calmodulin upon illumination by UV light. Like wild-type CaMKII, the L308BzF mutant stoichiometrically binds to Calmodulin, in a calcium-dependent manner. Using this construct, we demonstrate that Calmodulin binding to CaMKII, even under these stoichiometric conditions, does not perturb the CaMKII oligomeric state. Furthermore, we were able to achieve activation of CaMKII L308BzF by UV-induced binding of Calmodulin, which, once established, is further insensitive to calcium depletion. In addition to the canonical auto-inhibitory role of the regulatory segment, inter-subunit crosslinking in the absence of CaM indicates that kinase domains and regulatory segments are substantially mobile in basal conditions. Characterization of CaMKII^{L308BzF} in vitro, and its expression in mammalian cells, suggests it could be a promising candidate for control of CaMKII activity in mammalian cells with light.

KEYWORDS

calcium, crosslinking, kinase, UV

1 | INTRODUCTION

Many ion channels, enzymes, and signaling proteins connect to calcium signaling by binding the small calcium-binding protein Calmodulin. Calcium binds to Calmodulin at four sites, allowing it to expose hydrophobic pockets on its paired EF-hand motifs, and envelop

binding motifs on its target proteins (Chin & Means, 2000; Jurado et al., 2022). One of Calmodulin's best-studied targets is Ca²⁺-Calmodulin-dependent protein kinase II (CaMKII; Herring & Nicoll, 2016; Nicoll, 2017; Incontro et al., 2018).

CaMKII isozymes ($\alpha, \beta, \gamma, \delta$) regulate a plethora of cellular processes, including myocardial signaling and

This is an open access article under the terms of the [Creative Commons Attribution-NonCommercial](https://creativecommons.org/licenses/by-nc/4.0/) License, which permits use, distribution and reproduction in any medium, provided the original work is properly cited and is not used for commercial purposes.

© 2023 The Authors. *Protein Science* published by Wiley Periodicals LLC on behalf of The Protein Society.

neuronal plasticity involved in learning and memory (Takemoto-Kimura et al., 2017). A unique feature of this kinase is that it is organized as a dodecameric holoenzyme, made out of 12 subunit monomers. Each monomer of CaMKII comprises an N-terminal Serine/Threonine kinase domain, followed by a regulatory domain, a linker

region, and an association or “hub” domain (Figure 1a), which mediates self-oligomerization (Chao et al., 2011; Myers et al., 2017). In basal conditions, CaMKII is thought to be inhibited through stable docking of its regulatory domain to the substrate binding site. Once Ca^{2+} enters the cell and binds to Calmodulin, Ca^{2+} -

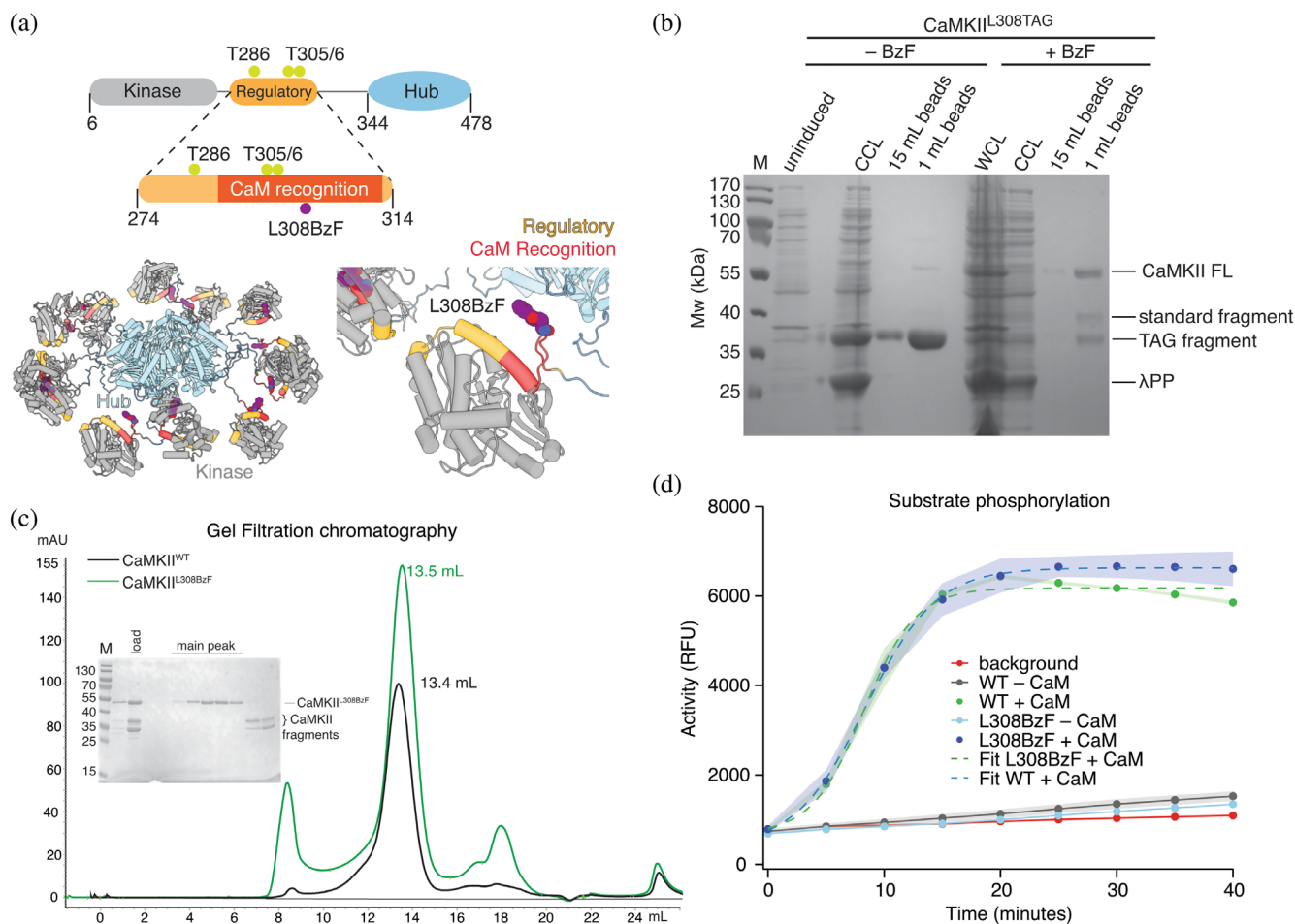


FIGURE 1 Characterization of CaMKII^{L308BzF}. (a) CaMKII domain arrangement showing N-terminal kinase domain (gray), followed by a regulatory domain (orange), a linker and a C-terminal association or hub domain (blue). Phosphorylation residues are colored in yellow (T286 and T305/306, CaMKII α numbering). Calmodulin recognition element is highlighted in red, and substitution of Leu at position 308 with BzF colored in purple. CaMKII holoenzyme is adapted using PDB:5U6Y. Cartoon representation of the CaMKII dodecamer with L308BzF residues colored purple and represented in spheres. (b) Coomassie-stained SDS-polyacrylamide gel showing rescue of CaMKII^{L308TAG} expression by growing *E. coli* in BzF-containing medium. Uninduced—uninduced culture; WCL—whole cell lysate; CCL—cleared cell lysate; 15 mL beads—sample from Co^{2+} beads resuspended in 15 mL of wash buffer, 1 mL beads—same volume of sample from 1 mL Co^{2+} beads resuspended in 1 mL of wash buffer; CaMKII FL—full-length CaMKII; λPP—Lambda Protein Phosphatase. (c) Chromatogram showing absorbance at 280 nm (mAU) from Superose 6 10/300 size exclusion run of purified CaMKII^{L308BzF}. An equivalent run for CaMKII^{WT} is shown for comparison. The first peak with elution volume (V_e) of 13.5 mL corresponds to dodecameric CaMKII holoenzyme (around 650 kDa). The second two peaks ($V_e = 17.2$ and 18.2 mL) correspond to smaller fragments of CaMKII. SDS gel shows the full length and fragments in different fractions from CaMKII^{L308BzF} run, as well as the sample loaded on the column (“load”). (d) Activity of CaMKII^{WT} (green line) and CaMKII^{L308BzF} (blue line) against CaMKII peptide-substrate (Syntide), measured using ADPQuest kinase assay, showing comparable $t_{1/2}$ for the two proteins. Red line—background signal, light green—CaMKII^{WT} activity in the absence of Ca^{2+} /CaM, light blue—CaMKII^{L308BzF} activity in the absence of Ca^{2+} /CaM. RFU—raw fluorescent units. The shading represents standard deviation (SD) from the mean value of three technical replicates.

calmodulin targets the regulatory domain of CaMKII and activates it by promoting an order-to-disorder transition of the inhibitory helix in the regulatory domain, which in turn frees the substrate binding site (Rellos et al., 2010). Subsequent trans-autophosphorylation at residue T286 (CaMKII α numbering), in the regulatory domain, adjacent to the Ca²⁺-calmodulin binding site, is enough to prevent rebinding of the regulatory domain to the substrate binding site. In principle and according to consensus models, CaMKII no longer requires Ca²⁺-calmodulin for its activity, and it remains active even after the initial Ca²⁺ stimulus has returned to baseline. In other words, calcium activation converts CaMKII from a Ca²⁺-triggered kinase into a constitutively-active enzyme. This bistable molecular switching of CaMKII action, referred to as autonomous activity (Chang et al., 2017; Lee et al., 2022; Tao et al., 2021), has made CaMKII an attractive candidate for a “memory molecule” in neuronal signaling (Lisman et al., 2002; Crick, 1984; Rossetti et al., 2017).

Other proteins, including kinases that are activated downstream of Ca²⁺ signaling, like PKC (Bear et al., 2018; Colgan et al., 2018), are proposed to be involved in synaptic plasticity, by altering cytoskeletal structure and receptor trafficking cycles. On the other hand, CaMKII is terrifically abundant in neurons and may have roles in addition to its enzymatic activity (like bundling actin; Okamoto et al., 2007; Kim et al., 2016). Particularly intriguing is the possibility that CaMKII alone could induce plasticity, in the absence of a substantial calcium signal, if it could be activated by a parallel means. To understand the specific role and biophysical mechanisms of CaMKII in calcium-triggered plasticity and memory, we sought to find a way to specifically activate CaMKII without calcium. To do this without the use of chemical activators or perturbing its structure by inserting large photo-responsive domains (Shibata et al., 2021), we exploited genetically-encoded unnatural amino acid mutagenesis, which we have previously used extensively in AMPA-type glutamate receptor ion channels in mammalian cells (Klippenstein et al., 2014; Poulsen et al., 2019) and more recently in CaMKII itself (Lučić et al., 2023). Using BzF (also known as Bpa), a well-studied UV-activated photocrosslinker (Nikić-Spiegel, 2020), we targeted the Calmodulin-binding footprint, aiming to irreversibly attach Calmodulin to CaMKII with light and maintain activity of the holoenzyme. Here we present in vitro characterization of this approach. Our results demonstrate that mutants that covalently trap Calmodulin on its cognate regulatory domains could offer spatial-temporal control of CaMKII activation and the activity of other targets of Calmodulin in mammalian cells.

2 | RESULTS AND DISCUSSION

2.1 | Characterization of CaMKII^{L308BzF}

In order to activate CaMKII α , from here on referred to as CaMKII, by UV-induced crosslinking, we designed a mutant of CaMKII in which we replaced the leucine residue at position 308, in calmodulin-binding R3 element of the regulatory domain, with the photoreactive unnatural amino acid benzoyl-L-phenylalanine (BzF; Figure 1a). To achieve this, we first introduced an amber stop codon (TAG) in place of the leucine codon (CTG) by site-directed mutagenesis. To incorporate BzF in the CaMKII protein, we co-expressed CaMKII TAG-containing plasmid, together with an orthogonal tRNA, mutated to recognize the TAG codon, and aminoacyl tRNA synthetase (aaRS) which attaches BzF to the cognate tRNA (for detailed procedure see Section 4.2). Only *E. coli* that was grown in BzF-containing medium expressed full-length CaMKII (Figure 1b) from this construct, demonstrating that there was no substantial leaky expression of full-length “wild-type” CaMKII, caused by TAG stop codon readthrough. A minor protein band corresponding to full-length CaMKII was visible also in expression conditions without BzF. The rescue of full-length CaMKII^{TAG} with BzF was not complete, because there was still a detectable fraction of truncated CaMKII, but the full-length CaMKII^{L308BzF} protein could be easily separated from the smaller fragments by size-exclusion chromatography. CaMKII^{L308BzF} had an elution volume similar to CaMKII^{WT} ($V_e = 13.5$ mL; Figure 1c), which corresponds well to the dodecameric holoenzyme elution profile of CaMKII^{WT}. Furthermore, the kinase activity of CaMKII^{L308BzF} toward a peptide-substrate, measured using ADPQuest kinase assay, was no different to CaMKII^{WT} (Figure 1d). The half-maximum time for peptide-substrate phosphorylation was about 8 min, similar to previous kinase activity of CaMKII measured in this way (Lučić et al., 2023). The reaction was complete in about 20 min. Given the 500-fold excess of substrate, this roughly corresponds to k_{cat} (per kinase domain) of about 0.5 s^{-1} ($500/1200 \text{ s}$) in our conditions. However, this estimate of k_{cat} was measured at only one ratio of enzyme to substrate concentration and is therefore subject to a high uncertainty.

Both CaMKII^{WT} and CaMKII^{L308BzF} proteins were subjected to Intact Mass Spectrometry (Figure S1). Measured mass difference between the two proteins closely resembles the mass difference between residues L and BzF ($\Delta m = 138$ Da). Some impurities, of lower molecular weights, are detected in the mass spectra of CaMKII^{L308BzF}, possibly due to poor separation of the full length CaMKII^{L308BzF} from truncated fragments during

size exclusion chromatography, which is not readily visible on an SDS-PAGE gel (Figure 1c). To our knowledge, CaMKII is the largest protein assembly successfully expressed with this technology.

We have also tested the rescue of CaMKII^{L308TAG} in mammalian HEK cells (Figure S2). In a cellular environment, both the rescued CaMKII with L308BzF and the truncated form (L308Stop) are produced. The rescue protocol requires further optimization in order to obtain more full-length CaMKII and less L308Stop protein product. For example, adding more BzF to the expression medium had a negative effect—it reduced the efficiency of the TAG codon rescue (Figure S2). However, the truncation at L308 should produce an enzyme that lacks Ca²⁺-stimulated activity, because the Calmodulin-binding site is disrupted by the truncation. Indeed, we

can observe a lack of phosphorylation at residue T286 on L308Stop in HEK cells (Figure S2), whereas the phosphorylation on the full-length CaMKII^{L308BzF} still occurs.

2.2 | UV-induced crosslinking of Calmodulin to CaMKII^{L308BzF} is Ca²⁺-dependent

Next, we examined whether CaMKII^{L308BzF} could be crosslinked to Calmodulin by UV light (Figure 2). The crosslinking induced by UV light is a covalent modification (Klán et al., 2013), unaffected by standard denaturing SDS-PAGE running conditions. Therefore, the formation of crosslinked complexes can be easily monitored with Coomassie staining of a polyacrylamide gel.

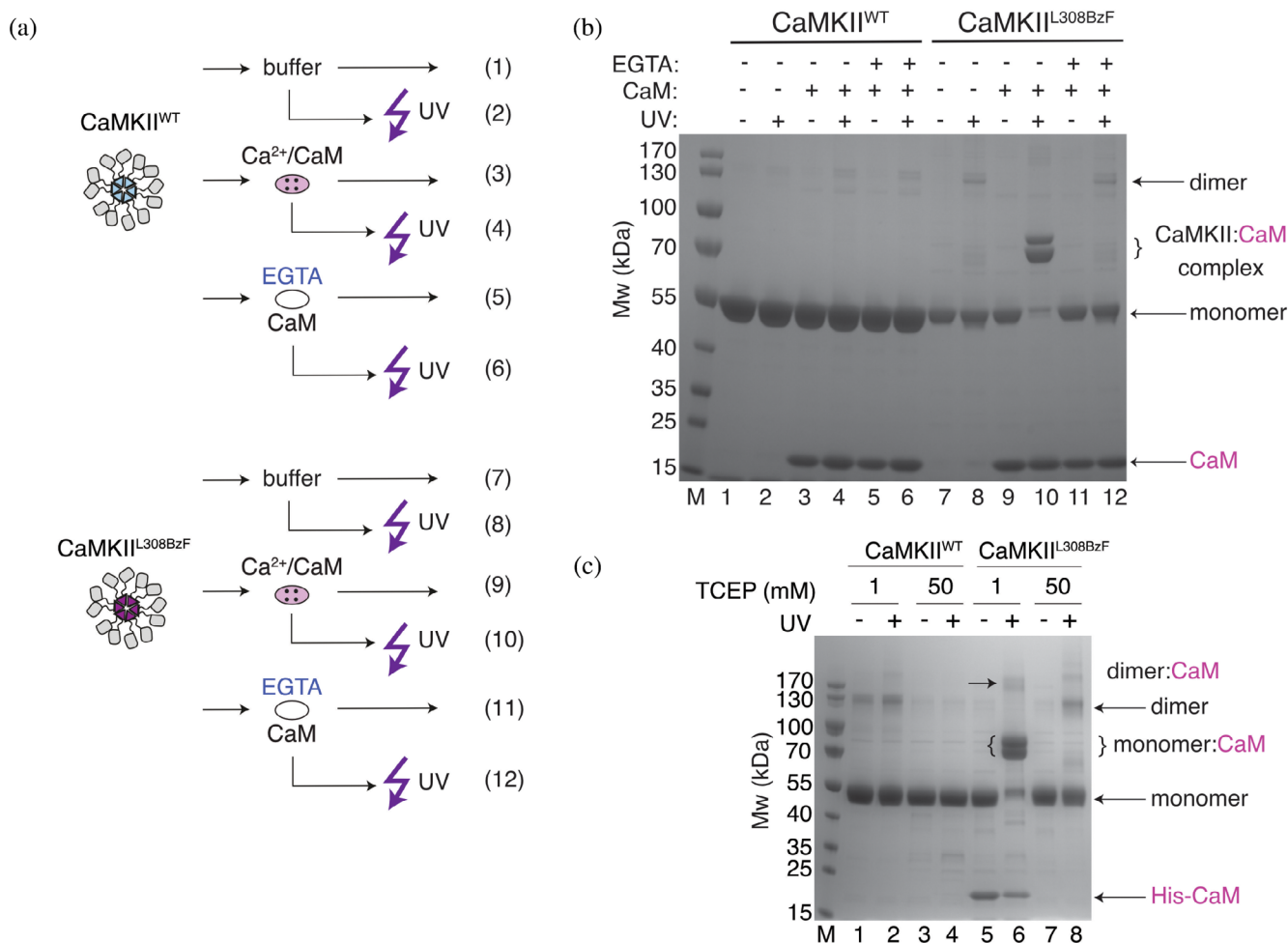


FIGURE 2 UV-induced crosslinking of Calmodulin to CaMKII^{L308BzF} is Ca²⁺-dependent. (a) Schematic representation of the experiment done in (b). (b) Coomassie-stained SDS-polyacrylamide gel showing absence of UV-induced crosslinking of Calmodulin to CaMKII^{WT} (first 6 lanes), and dependence of UV-induced crosslinking of Calmodulin to CaMKII^{L308BzF} on Ca²⁺ (second 6 lanes). CaM—Calmodulin. (c) Coomassie-stained SDS-polyacrylamide gel showing UV-induced CaMKII dimer formation when 1 mM TCEP is used in the CaMKII buffer (lanes 1, 2, 5, and 6) and absence of this band when the CaMKII buffer is supplemented with 50 mM TCEP in the case of CaMKII^{WT} (lanes 3 and 4), but not in the case of CaMKII^{L308BzF} (lane 8). His-tagged Calmodulin (His-CaM) is present in lanes 5 and 6.

To limit heat-induced denaturation and associated damage coming from the UV lamp exposure, we placed CaMKII samples in a passively cooled metal plate in a cold room (4°C) and treated the samples with light of 365 nm wave-length (see Section 4.6 for details). In order to mimic the high cellular concentration of CaMKII (Otmakhov & Lisman, 2012), we used 8 μM CaMKII and different concentrations of Calmodulin. Figure 2a shows a schematic representation of experiments performed in Figure 2b. Treatment of CaMKII^{L308BzF} with UV light in the presence of Calmodulin caused a nearly complete protein band shift on a denaturing SDS-polyacrylamide gel to higher molecular weight (Mw; from 55 to 70 kDa), corresponding to the combined mass of CaMKII monomer (55 kDa) and Calmodulin (17 kDa) (Figure 2b, lane 10). The depletion of vast majority of the 55 kDa band suggests stoichiometric crosslinking, indicative of a tight interaction. The remaining signal detected in the monomeric band (around 5%, Figure 2b, lane 10) might lack the BzF residue at position L308, due to minor leaky expression of this construct, as seen in Figure 1b. The shift was absent when we used CaMKII^{WT} protein (Figure 2b, lane 4), showing that the cross-linking observed on the gel was specific to BzF residue at position 308 and Calmodulin. Furthermore, the crosslinking was absent if Calmodulin was previously stripped of Ca²⁺ by EGTA treatment (Figure 2b, lane 12), demonstrating that the complete reaction was dependent on the correct conformation of Calmodulin.

In CaMKII^{WT} samples, a band corresponding to the CaMKII dimer appeared after UV treatment. This band was absent when we diluted CaMKII in a buffer containing 50 mM TCEP, instead of our standard buffer which contained 1 mM TCEP (Figure 2c), indicative of the exposure of free cysteines, perhaps by sample heating or denaturation, which then allows nonspecific dimers of CaMKII to form. Although the double band appearing when CaMKII^{L308BzF} is crosslinked to Calmodulin could be explained by additional linking of the Cysteines in proximity of the residue 308 (Cys at position 280 or 289; Torres-Ocampo et al., 2020), which might be promoted more in CaMKII^{L308BzF} than in CaMKII^{WT} dimer, this double band persisted in 50 mM TCEP. Notably, following UV treatment of CaMKII^{L308BzF} alone (without Calmodulin), and in the presence of 50 mM TCEP (Figure 2c, lane 8), dimeric and higher order bands of CaMKII^{L308BzF} appeared, although this band is reduced in CaMKII^{WT} under the same conditions (Figure 2c, lane 4). If we interpret this observation as inter-subunit covalent crosslinking by the L308BzF residue, the question arises, how is this possible if the regulatory segment is always docked in basal conditions? These higher-order bands suggest that in the complete absence of CaM, the

regulatory segment of CaMKII is mobile enough to contact other monomers, and is not persistently docked, which agrees well with previously published work on CaMKII dynamics (Hoffman et al., 2011). In this interpretation, in the presence of Calcium-Calmodulin, regulatory segments, although undocked, are cloaked by bound Calmodulin and cannot make intersubunit crosslinks. Even though higher-order bands were generally a minor fraction, we used 50 mM TCEP in most subsequent experiments to limit the formation of disulfide-bonded higher-order oligomers upon denaturation.

To further investigate the origin of the double band in CaMKII samples, we performed mass spectrometry analysis on CaMKII^{L308BzF} under several conditions (Figure S3). The analysis showed that, when exposed to UV light, CaMKII undergoes disulfide bridging on Cysteine 280 in the regulatory domain (Figure S3C). This was determined by treating CaMKII samples with an alkylation reagent (chloroacetamide; CAA) which binds only to free Cysteines resulting in carbamidomethyl modification (Giron et al., 2011; Goodman et al., 2018). We calculated the ratio of intensities between peptides with carbamidomethyl modification (free Cysteines) over unmodified peptides (disulfide bridged). We took 24 gel samples corresponding to four replicates of six gel bands (these six were drawn from four conditions; each condition is a lane run on the gel; Figure S3). Four of these samples (CaMKII^{L308BzF}, CaMKII^{L308BzF} UV treated, CaMKII^{L308BzF} incubated with Ca²⁺:Calmodulin, and CaMKII^{L308BzF} incubated with Ca²⁺:Calmodulin and UV treated—lower band from the doublet at 70 kDa) showed modification on Cys280 corresponding to Cys280 being free (Figure S3C), that is, not disulfide-bonded. However, we found that a portion of the sample of CaMKII^{L308BzF} incubated with Calmodulin and then treated with UV had a ratio of modified to base intensity ($I_{\text{modified}}/I_{\text{base}}$) very close to 0 (due to very little or no modification; Figure S3B). The upper of the doublet band around 70 kDa in CaMKII^{L308BzF} incubated with Calmodulin and then UV treated, and the uncrosslinked band from the same condition (corresponding to CaMKII monomer), both show $I_{\text{modified}}/I_{\text{base}}$ equal to or close to 0, indicative of absence of carbamidomethyl modification. This absence of modification is likely caused by Cysteine 280 forming a disulfide bridge with another Cysteine in the vicinity. A similar pattern was found also for Cysteine 289, but the coverage for this peptide was not substantial, and it was not identified in all 4 replicates of each sample. We could also not confirm BzF incorporation in individual bands because of poor coverage. We did not test the double bands appearing at around 120 kDa corresponding to CaMKII dimers, but we suspect that they are also the result of similar disulfide bridging.

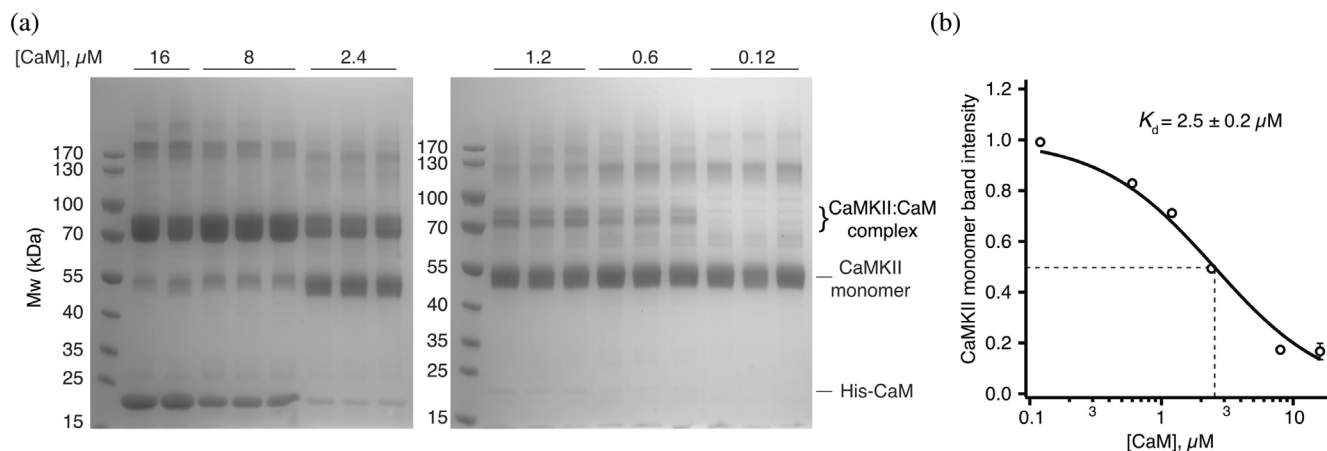


FIGURE 3 Determination of Calmodulin binding constant. (a) Coomassie-stained SDS-polyacrylamide gel of samples containing CaMKII^{L308BzF} and varying concentrations of His-Calmodulin (0.12–16 μM) supplemented with 2 mM CaCl₂, used to quantify UV-dependent CaMKII^{L308BzF} monomer band depletion, used to construct the binding curve in panel (b). CaM—Calmodulin. (b) Calculation of Calmodulin dissociation constant (k_d), by fitting the densitometry of Calmodulin and UV-dependent depletion of monomeric CaMKII^{L308BzF} bands from the gels in panel (a).

Using UV-induced cross-linking we were able to determine the binding constant of Calmodulin to CaMKII^{L308BzF}. A total of 8 μM CaMKII^{L308BzF} was incubated with different concentrations of Calmodulin (16, 8, 2.4, 1.2, 0.6, and 0.12 μM) in triplicate, and each reaction was exposed to UV, followed by SDS-PAGE analysis. By measuring CaMKII monomer band densitometry from Coomassie-stained gel, we found that UV-induced cross-linking of Calmodulin to CaMKII depletes the CaMKII monomer band, as a result of shifting to the Ca²⁺:Calmodulin:CaMKII^{L308BzF} complex, with K_D of $2.5 \pm 0.2 \mu\text{M}$ (Figure 3). Despite being measured in a completely different way, and despite the very strong dependence of association on calcium concentration, this affinity is not starkly different from the previously reported affinity (0.6 μM) of Calmodulin to CaMKII α from ITC measurements (Rellos et al., 2010), suggesting that the incorporation of BzF at position 308 does not alter the association of the CaMKII:CaM complex much.

2.3 | Calmodulin binding does not change oligomeric state of CaMKII^{L308BzF}

It has been proposed that binding of Ca²⁺:Calmodulin during CaMKII activation causes the release of subunits from the dodecameric CaMKII holoenzyme (Bhattacharyya et al., 2016; Karandur et al., 2020; Stratton et al., 2014). We wanted to directly test the effect of Ca²⁺:Calmodulin binding alone to CaMKII holoenzymes on the oligomeric state of CaMKII^{L308BzF}. The advantage of our approach is that we get almost 100% of CaMKII^{L308BzF} crosslinked to Calmodulin upon UV

exposure, so any effect that Calmodulin might exert on oligomeric state of CaMKII should not be masked by incomplete binding. To this end, we employed mass photometry (Figure 4), a single molecule technique that measures light scattered from mobile particles in solution as they make transient contact a coverslip, enabling calculation of their Mw (Young et al., 2018). Detected particles are described as counts on the y-axis of the graphs in Figures 4, S4, and S5. The measurements were performed in triplicate (Figures S4 and S5), demonstrating good reproducibility between measurements. We tested three different concentrations of CaMKII (400, 100, and 10 nM). CaMKII formed dodecameric holoenzymes even at the lowest concentration, 10 nM (Figure S4D). In all measured conditions and at all concentrations, a small peak corresponding to monomer-dimer CaMKII was detected, assuring that the instrument can indeed detect smaller particles. In some of the measurements, a peak at negative Mw values appeared, which corresponds to particle unbinding events. However, this peak was, if there, always a minor fraction (2%–5%). We also reported sigma values for each peak, which correspond to peak width and inform us about the distribution of the particles' sizes.

After mass photometry, each sample was run on SDS-PAGE to validate the reactions (Figure S4F). Two different batches of purified CaMKII^{L308BzF} were compared, as well as two different Calmodulins (self-made and commercial, purchased from Calbiochem). The electrophoresis results were similar between all combinations of CaMKII and Calmodulin (Figure S4F).

We first measured isolated CaMKII^{WT} protein (Figure 4a), and compared it to either CaMKII^{WT}

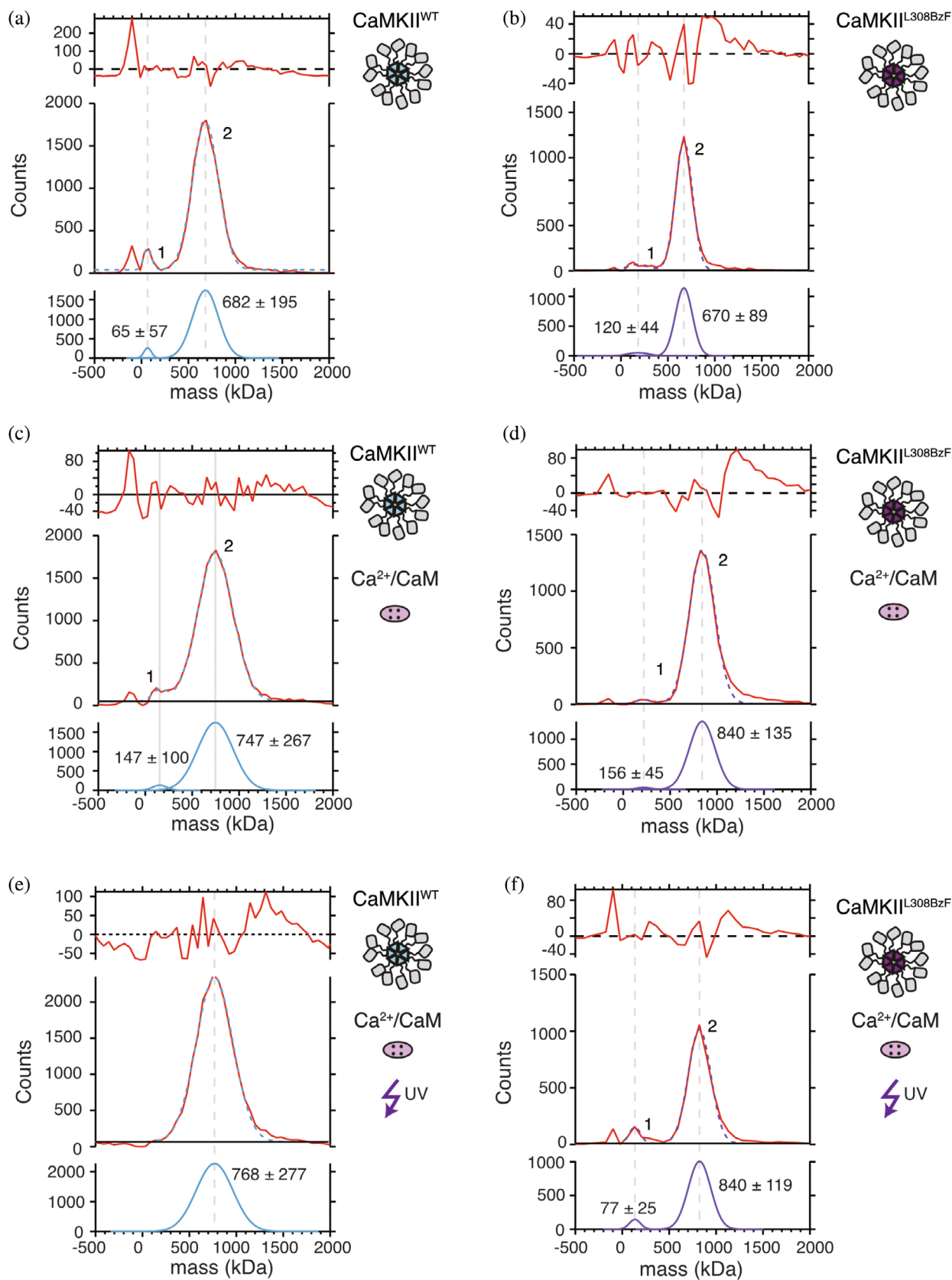


FIGURE 4 Legend on next page.

incubated with Ca^{2+} :Calmodulin in the absence (Figure 4c) or presence of UV light (Figure 4e), as well as to CaMKII^{L308BzF} alone (Figure 4b), CaMKII^{L308BzF} incubated with Ca^{2+} :Calmodulin in the absence (Figure 4d) or presence of UV light (Figure 4f). The concentration of all CaMKII proteins was initially set to 8 μM and Calmodulin to 8 μM . Selected samples were then treated with UV light, and the concentration of all samples was diluted to 400 nM (CaMKII monomer concentration) in the measured drop on the instrument, because particles were too dense at higher concentrations, so the instrument could not distinguish them from one another.

Consistent with previous work (Lučić et al., 2023; Torres-Ocampo et al., 2020), particles of isolated CaMKII^{WT} (Figure 4a) gave a major peak with estimated Mw corresponding to dodecameric holoenzymes (Mw = 682 kDa), together with a smaller peak (around 1%–2%) corresponding to monomer-dimer Mw. Incubation of CaMKII^{WT} with Ca^{2+} :Calmodulin (Figure 4c) resulted in the appearance of a major peak with Mw = 747 kDa and a smaller shoulder peak (around 1%–2%) at the lower Mw, similar to that one seen in Figure 4a. The major peak corresponds to partially Calmodulin-bound dodecamers ($12 \times 55 \text{ kDa} + 5 \times 16.4 \text{ kDa} = 742 \text{ kDa}$). We cannot exclude that other combinations of CaMKII:CaM would give a similar Mw (e.g., a decamer with 10 CaM bound would be $\sim 720 \text{ kDa}$). Nonetheless, there is no major monomer-dimer peak detected upon incubation with Calmodulin. Treatment of Ca^{2+} :Calmodulin and CaMKII^{WT} mixture with UV resulted in a single peak of Mw = 768 kDa, which would correspond to one holoenzyme of CaMKII with 6 Ca^{2+} :Calmodulin bound ($12 \times 55 \text{ kDa} + 6 \times 16.4 \text{ kDa} = 758 \text{ kDa}$) (Figure 4e), similar to the untreated CaMKII^{WT} sample.

Particles coming from CaMKII^{L308BzF} alone were measured to have similar Mw (670 kDa) like the CaMKII^{WT} (Figure 4b) as expected. Again, a small peak (1%–2%) corresponding to CaMKII dimer size (120 kDa) was detected. Detected size of CaMKII^{L308BzF} in the presence of Calmodulin, but without UV treatment (Figure 4d; Mw = 840 kDa), corresponds to fully Calmodulin-bound

CaMKII^{L308BzF} ($12 \times 55 \text{ kDa} + 12 \times 16.4 \text{ kDa} = 855 \text{ kDa}$). This discrepancy between particle sizes of CaMKII^{WT} and CaMKII^{L308BzF} incubated with Calmodulin could come from different Calmodulin concentrations used in these experiments (2 μM Calmodulin with CaMKII^{WT}, and 8 μM Calmodulin with CaMKII^{L308BzF}). However, when we compared CaMKII^{WT} (Figure 4c, e) to CaMKII^{L308BzF} using the same Calmodulin (Figure S5E, F), the difference was absent. A small dimeric peak (Mw = 156 kDa) preceding the main peak (Figure 4d) is still in small abundance (around 1%–2%) similar to the one measured in the condition in Figure 4b, and could have Calmodulin bound to it ($55 \text{ kDa} \times 2 + 16.4 \text{ kDa} \times 2 = 143 \text{ kDa}$). It is expected that dimers which dissociate from holoenzymes due to concentration-dependent dissociation are still capable of binding to Calmodulin. Irreversible crosslinking of CaMKII^{L308BzF}:Calmodulin mixtures with UV light did not further change the stoichiometry of CaMKII^{L308BzF} holoenzymes (Figure 4f; Mw = 840 kDa).

Perhaps contrary to expectation, under the conditions used here, we failed to detect particles corresponding in size to dissociated CaMKII subunits dependent on Calmodulin presence. It is possible that holoenzymes did not dissociate because we omitted ATP from these measurements. Therefore, trans-autophosphorylation of the regulatory domain, which might be necessary for the disassembly of holoenzymes (Bhattacharyya et al., 2016; Karandur et al., 2020), was not promoted. However, these results show that Calmodulin binding to CaMKII in and of itself, does not break up the CaMKII holoenzyme, even when the binding is stoichiometric, and irreversible like in the case of UV-treated CaMKII^{L308BzF}: Ca^{2+} :Calmodulin mixture (Figure 4f).

2.4 | Ca^{2+} is dispensable for the activity of constitutively calmodulin bound CaMKII

Binding of Ca^{2+} -bound Calmodulin to CaMKII is the first step in the activation of CaMKII, and it is necessary to

FIGURE 4 UV-induced crosslinking of Calmodulin to CaMKII^{L308BzF} does not change the oligomeric state of CaMKII. (a) Mass distribution of 400 nM CaMKII^{WT} under resting conditions. The distribution consists of 7161 particle mass measurements (total counts). (b) Mass distribution of 400 nM CaMKII^{L308BzF} under resting conditions (6138 total counts). (c) Mass distribution of 400 nM CaMKII^{WT} incubated with Ca^{2+} :Calmodulin (20,440 total counts). (d) Mass distribution of 400 nM CaMKII^{L308BzF} incubated with Ca^{2+} :Calmodulin (8154 total counts). (e) Mass distribution of 400 nM CaMKII^{WT} incubated with Ca^{2+} :Calmodulin and UV-treated (24,153 total counts). (f) Mass distribution of 400 nM CaMKII^{L308BzF} incubated with Ca^{2+} :Calmodulin, and UV-treated (4964 total counts). Graph top panels—residuals of the Gaussian fit (red); middle panels—histogram of the counts (red line) with fitted Gaussian curve (dashed blue line for CaMKII^{WT}, dashed magenta line for CaMKII^{L308BzF}), bottom panels—Gaussian fits of the counts (blue line—CaMKII^{WT}, magenta line—CaMKII^{L308BzF}). The centers and widths of the fitted peaks are indicated.

relieve the inhibition posed by the regulatory domain, which otherwise obstructs the substrate binding cleft in naïve CaMKII (Rellos et al., 2010; Shifman et al., 2006). In order to bind to CaMKII, we would expect that Calmodulin should adopt the correct conformation, which is obtained by Ca^{2+} binding (Shifman et al., 2006). Only when Ca^{2+} :Calmodulin is bound to the regulatory domain, can CaMKII trans-autophosphorylate itself at position T286, at which point CaMKII no longer needs Ca^{2+} :Calmodulin because phosphorylation at T286 prevents rebinding of the regulatory domain to the substrate binding cleft, and CaMKII can now freely engage its substrates (Rellos et al., 2010). This Ca^{2+} :Calmodulin-independent state is known as autonomous activity of CaMKII (Lee et al., 2022).

The mutant CaMKII^{L308BzF} allowed us to ask whether CaMKII can be switched into autonomous activity (synonymous with ongoing T286 phosphorylation) in very low calcium. To do this, we performed experiments in high, intermediate, and very low free calcium concentrations (2 mM, 26 nM, and 540 pM; using 7 and 40 mM EGTA for the second and third conditions, free Calcium was calculated with MaxChelator). These results are shown in Figures 5 and S3. For clarity, Figure 5a shows schematic representations of the experiments performed in Figure 5b (likewise in Figure S6). Incubation of mixtures containing Ca^{2+} :Calmodulin and CaMKII^{L308BzF} with EGTA, prior to UV treatment, was sufficient to abolish CaMKII^{L308BzF}:Calmodulin crosslinking (Figures 2b, 5b; top panel, lane 10; Figure S6B, top panel, lane 14). Minor phosphorylation signals could still be detected, albeit at about 20–30× less intensity, on these CaMKII^{L308BzF} species, as well as on CaMKII^{WT} without UV treatment (Figure 5b, middle panel, lane 10, lanes 3 and 4; Figure S6B lanes 3 and 4) but this was not consistent (Figure S6B, middle panel, lanes 14 and 15). These results indicate that there is almost no interaction between Calmodulin and regulatory domain of CaMKII in the presence of Ca^{2+} chelating agent, and therefore, at most a very small portion of trans-autophosphorylation. However, if we first treated the mixtures of Ca^{2+} :Calmodulin and CaMKII^{L308BzF} with UV, and then added EGTA (Figure 5b, lane 12; Figure S6B, lane 16), the phosphorylation signal was strong and indistinguishable to samples that were never exposed to EGTA (Figure 5b, lane 9; Figure S6B lane 12). This observation means that the crosslinking of Ca^{2+} :Calmodulin to CaMKII^{L308BzF} either prevents stripping of Ca^{2+} from Calmodulin or simply enables tight binding of Calmodulin to the regulatory domain of CaMKII, perhaps independent of Calmodulin conformation. In any case, this crosslinking switched CaMKII to calcium-independent phosphorylation of T286, resembling autonomous activity.

Additionally, pre-incubation of Calmodulin with CaMKII might enhance Calmodulin affinity for Ca^{2+} , as has been previously reported (Shifman et al., 2006), making it more difficult to chelate Ca^{2+} ions with EGTA. Incubation of premixed CaMKII and Ca^{2+} :Calmodulin with a high amount of EGTA ($[\text{EGTA}]:[\text{Ca}^{2+}] = 20$) prior to UV treatment, still allowed for residual phosphorylation on T286 in mixtures that were subsequently UV treated (Figure 5B, middle panel, lane 10), but if the mixture was not subsequently subjected to UV, the phosphorylation signal was completely abolished (Figure 5b, middle panel, lane 11). This result further indicates that our UV-sensitive mutant can capture a tiny residual proportion of tightly-bound CaM in nominally ultra-low calcium and that this is sufficient to allow phosphorylation (note, pre-stripping CaM of calcium was more effective at stopping phosphorylation). Incubation of Ca^{2+} :Calmodulin with EGTA prior to addition to CaMKII^{L308BzF} was sufficient to prevent Calmodulin:CaMKII^{L308BzF} crosslinking (Figure 5B, top panel, lanes 13 and 14; Figure S6B, top panel, lanes 17 and 18), although it allowed UV-dependent formation of higher-order CaMKII oligomers, as in Figure 2, likely due to interaction of regulatory domain of CaMKII of one monomer to the regulatory or kinase domain of CaMKII of adjacent monomers (Chao et al., 2010; Rocco-machado et al., 2022). This result further indicates that domains within the dodecamer are mobile, making dynamic intersubunit contacts, and also perhaps that the regulatory segment is not permanently docked on the substrate binding site of its parent subunit (Hoffman et al., 2011).

The phospho-signal was absent when Ca^{2+} :Calmodulin was pre-incubated with high EGTA (20-fold excess, Figure 5b, middle panel, lane 14; Figure S6B, middle panel lane 18), due to efficient chelation of Ca^{2+} . On the other hand, pre-incubation of Ca^{2+} :Calmodulin with EGTA in 3.5-fold excess of Ca^{2+} was not sufficient to completely abolish phosphorylation of CaMKII^{L308BzF} (Figure 5b, middle panel, lane 13; Figure S6B, middle panel, lane 17). Similar results were obtained with the wt protein (Figure 5b, middle panel, lanes 3 and 4; Figure S6B, middle panel, lanes 3 and 4), although in this case incubation of CaMKII^{WT} with the same Ca^{2+} :Calmodulin:EGTA mixture (see Section 4.9 for details) with a 20-fold excess of EGTA to Ca^{2+} still did not completely abolish the phosphorylation signal (Figure 5b, middle panel, lanes 5 and 6; Figure S6B, middle panel, lane 5), although it was reduced 80-fold, compared to EGTA untreated sample (Figure 5b, middle panel, lane 1). However, we cannot exclude the possibility that residual binding of free Mg^{2+} ions (we had 15 and 1.3 mM free Mg^{2+} in the presence of 7 and 40 mM EGTA, respectively; calculated with MaxChelator) to Calmodulin in these

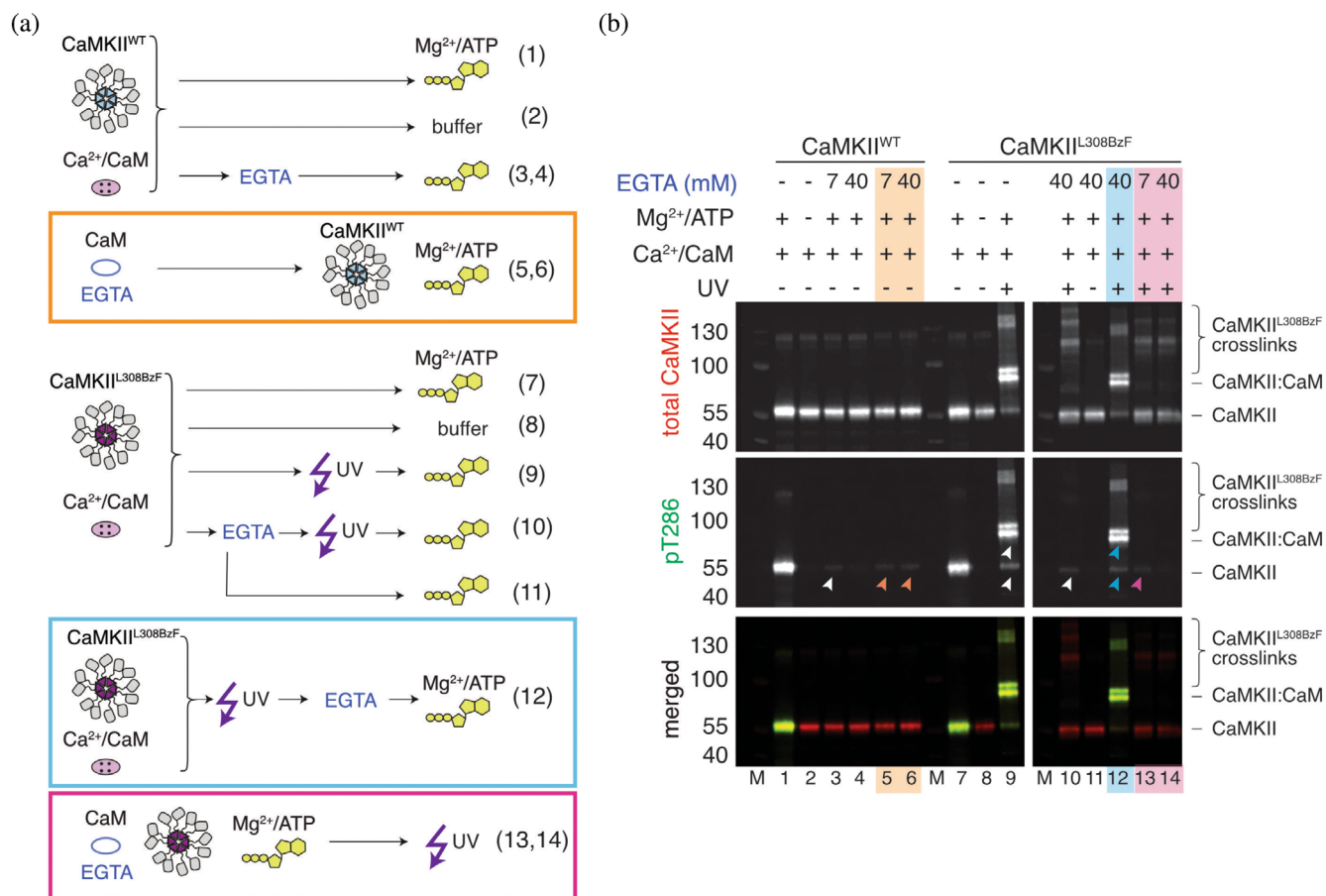


FIGURE 5 Ca²⁺ is dispensable for the activity of constitutively Calmodulin-bound CaMKII. (a) Schematic representation of experiments done in (b). (b) Western blot detection of the ability of CaMKII^{WT} (first 6 lanes) or CaMKII^{L308BzF} (second 8 lanes) to trans-autophosphorylate itself under different conditions. Lane 1—CaMKII^{WT} activated with Ca²⁺:CaM, and then incubated with Mg²⁺:ATP for 10 min at 37°C; lane 2—CaMKII^{WT} activated with Ca²⁺:CaM, and then incubated with SEC buffer instead of Mg²⁺:ATP, for 10 min at 37°C; lane 3—CaMKII^{WT} activated with Ca²⁺:CaM, followed by incubation with 7 mM EGTA, and then incubated with Mg²⁺:ATP for 10 min at 37°C; lane 4—CaMKII^{WT} activated with Ca²⁺:CaM, followed by incubation with 40 mM EGTA, and then incubated with Mg²⁺:ATP for 10 min at 37°C; lane 5—CaMKII^{WT} incubated with Ca²⁺:CaM, which was treated with 7 mM EGTA prior to incubation with CaMKII, followed by incubation with Mg²⁺:ATP for 10 min at 37°C; lane 6—CaMKII^{WT} incubated with Ca²⁺:CaM, which was treated with 40 mM EGTA prior to incubation with CaMKII, followed by incubation with Mg²⁺:ATP for 10 min at 37°C; M—marker; lane 7—CaMKII^{L308BzF} activated with Ca²⁺:CaM, and then incubated with Mg²⁺:ATP for 10 min at 37°C; lane 8—CaMKII^{L308BzF} activated with Ca²⁺:CaM, and then incubated with SEC buffer instead of Mg²⁺:ATP, for 10 min at 37°C; lane 9—CaMKII^{L308BzF} activated with Ca²⁺:CaM, followed by UV treatment, and then incubated with Mg²⁺:ATP for 10 min at 37°C; M—marker; lane 10—CaMKII^{L308BzF} activated with Ca²⁺:CaM, incubated with 40 mM EGTA, UV treated, and then incubated with Mg²⁺:ATP for 10 min at 37°C; lane 11—CaMKII^{L308BzF} activated with Ca²⁺:CaM, incubated with 40 mM EGTA, and then incubated with Mg²⁺:ATP for 10 min at 37°C; lane 12—CaMKII^{L308BzF} activated with Ca²⁺:CaM, UV treated, then incubated with 40 mM EGTA, and then incubated with Mg²⁺:ATP for 10 min at 37°C; lane 13—CaMKII^{L308BzF} incubated with Ca²⁺:CaM, which was treated with 7 mM EGTA prior to incubation with CaMKII, followed by incubation with Mg²⁺:ATP for 10 min at 37°C, and then UV treatment; lane 14—CaMKII^{L308BzF} incubated with Ca²⁺:CaM, which was treated with 40 mM EGTA prior to incubation with CaMKII, followed by incubation with Mg²⁺:ATP for 10 min at 37°C, and then UV treatment. Blue box indicates that UV treatment was preceding the EGTA treatment; orange box indicates that incubation of Ca²⁺:CaM with EGTA was preceding the incubation with CaMKII; purple box indicates that EGTA treatment and activation preceded UV treatment. Arrowheads on the blots represent pT286 signal in respective lanes. Green bands on the blot represent fluorescence of the secondary antibody recognizing pT286, while the red bands on the blot represent fluorescence of the secondary antibody recognizing total CaMKII protein.

reactions could somehow mediate its proper folding and therefore binding to CaMKII. The small discrepancy between CaMKII^{WT} and CaMKII^{L308BzF} levels of

phosphorylation in these reactions might arise from a modest difference in Calmodulin affinity between wt and L308BzF mutant, in which wt residue L on position

308 makes residual binding of Calmodulin possible and sufficient to drive low phosphorylation of T286 (80× lower than in EGTA untreated sample). Since the phosphorylation signal was completely absent in reactions where either ATP:Mg²⁺ was omitted from the reaction (Figure 5b lanes 2 and 8, Figure S6B lanes 2 and 11) or Ca²⁺:CaM (Figure S6B lanes 7 and 8), it is clear that residual phosphorylation occurring at ultra-low calcium is not a consequence of pre-existing phosphorylation on CaMKII which might have occurred in *E. coli* during expression.

3 | CONCLUSION

Using a photoactive unnatural amino acid as a tool for probing CaMKII:Calmodulin interaction, we could show that Calmodulin binding to CaMKII alone does not cause disassembly of the CaMKII holoenzyme (Figure 4). The CaMKII^{L308BzF} mutant, which maintained the stoichiometric binding characteristic of wild-type CaMKII, allowed the irreversible attachment of Calmodulin with UV-induced crosslinking. This crosslinked complex showed similar activity to the wild-type kinase, even under conditions of negligible free calcium. Our activity assays also revealed that a residual auto-phosphorylation of CaMKII is still present even when Calmodulin:CaMKII^{L308BzF} crosslinking is undetectable on western blot, indicating that a small amount of Calmodulin might remain constitutively bound to CaMKII. Finally, cross-linking of higher-order inter-subunit CaMKII complexes by L308BzF in the absence of CaM demonstrated that the regulatory segment is mobile in basal conditions.

Following from these observations, the CaMKII^{L308BzF} mutant could be a promising candidate for irreversible photo-activation of CaMKII in cells. However, the CaMKII L308Stop truncation may behave differently from native CaMKII in other ways, particularly as it lacks the hub domain. Nonetheless, this mutant might find utility as a complement to previous functional mutants of CaMKII that promoted constitutive activity, which also lacked the hub domain, and alternative methods for controlling CaMKII with light (Parra-bueno et al., 2017; Shibata et al., 2021). Such a tool might be used for acute activation of CaMKII, in order to promote processes like long-term potentiation of synaptic transmission in neurons with a high temporal precision. This application is particularly interesting in light of the recent data suggesting that CaMKII modification in the regulatory domain triggers plasticity, even in the absence of enzymatic function (Chen et al., 2023; Tullis et al., 2023).

4 | MATERIALS AND METHODS

4.1 | Expression constructs

Human *wild-type* CaMKII α (CaMKII^{WT}), with a 30 residue linker between regulatory and hub domains, was gene optimized for expression in *E. coli*, and the first 5 residues of the CaMKII α protein were deleted (Chao et al., 2011). A hexa-his tag was placed on the N-terminus, followed by TEV cleavage site, and synthesized by GenScript in pET28b + vector, flanked by NcoI and HindIII restriction sites. CaMKII^{L308BzF} was cloned over CaMKII^{WT} background using TAG-containing primers, by site-directed-mutagenesis. Human CaMKII^{WT}-mScarlet used for expression in mammalian cells was cloned by fusing the human CaMKII^{WT} gene purchased from Addgene (plasmid# 23408, ref; Johannessen et al., 2011) to mScarlet purchased from Addgene (plasmid# 85054, ref; Bindels et al., 2016), and the L308TAG site was introduced by site-directed-mutagenesis. Human Calmodulin with an N-terminal His₈ tag, followed by a TEV cleavage site, was codon optimized for expression in *E. coli* in pET28b + plasmid, and gene synthesized by GenScript. Lambda protein phosphatase (LPP) was purchased from Addgene (plasmid #79748; Albanese et al., 2018). The plasmid containing TEV protease was a kind gift from Prof. Dr. Thomas Leonard (Max Perutz Laboratories, Vienna, Austria). The plasmid containing aminoacyl synthetase (aaRS) and tRNA from *M. jannaschii* (Young et al., 2010) in pEVOL backbone, was a kind gift from Prof. Dr. Thomas Söllner (BZH, Heidelberg, Germany). Human Calmodulin with an N-terminal His₈ tag, followed by a TEV cleavage site, was codon-optimized for expression in *E. coli* and gene synthesized (GenScript) using pET28b + vector as a backbone. The BzF tRNA and RS for mammalian cell expression were a kind gift from Thomas Sakmar (Rockefeller; Ye et al., 2008).

4.2 | CaMKII expression

Expression of CaMKII^{WT} was done in BL21 *E. coli* cells, grown in LB medium. To aid solubility, CaMKII^{WT} (Kanamycin resistance) was co-expressed with LPP (Spectinomycin resistance). Cells were grown in LB medium at 37°C/200 rpm until OD₆₀₀ reached 1.2–1.5. Expression of both genes was induced by adding 0.4 mM IPTG, and the medium was supplemented with 0.5 mM MnCl₂ (co-factor of LPP). Protein expression was continued overnight at 20°C.

Expression of CaMKII^{L308BzF} was performed by co-expression of CaMKII^{L308TAG} (Kanamycin resistance),

LPP (Spectinomycin resistance), and a plasmid containing orthogonal aaRS and tRNA from *M. jannaschii* (Chloramphenicol resistance; Young et al., 2010) in *E. coli* BL21 cells. Cells were grown at 37°C/200 rpm in LB medium until they reached $OD_{600} = 0.6$. The medium was then supplemented with 1 mM BzF (BACHEM, product #4017646), and cells continued to grow for another 30 min. The temperature was then lowered to 30°C, and the aaRS and tRNA expression was induced by adding 15 mM arabinose. The cells continued to grow until the OD_{600} reached 1.2–1.5, the temperature was lowered to 20°C, and CaMKII^{L308TAG} and LPP expression was induced by addition of 0.4 mM IPTG. The medium was supplemented with 0.5 mM MnCl₂ and the cultures were grown overnight at 20°C.

4.3 | Calmodulin expression

Human Calmodulin (Kanamycin resistance) expression was performed in Rosetta DE3 cells (Chloramphenicol resistance) in a TB medium, supplemented with 5 mM CaCl₂. Protein expression was induced at $OD_{600} = 1.8$ by 1 mM IPTG. Cells were harvested after growing for 5 h at 37°C/200 rpm.

4.4 | CaMKII purification

Cell pellets expressing either CaMKII^{WT} or CaMKII^{L308BzF} were lysed in lysis buffer (50 mM Tris pH 8, 300 mM NaCl, 20 mM imidazole, 1 mM TCEP) supplemented with 0.02 mg/mL DNaseI, 5 mM MgCl₂, 0.5 mg/mL lysozyme and 1 mM PMSF. The lysates were additionally passed through a cell disruptor two times before the lysates were cleared of cell debris by centrifugation (16k rpm, 4°C). Both constructs have an N-terminal His₆ tag, which was used for affinity purification with 5 mL NiNTA column (GE Healthcare), previously equilibrated in Ni_A buffer (50 mM Tris pH 8, 300 mM NaCl, 20 mM imidazole, 1 mM TCEP). The column was then extensively washed (100 mL of Ni_A buffer, 50 mL of Ni_A buffer with 50 mM imidazole, 50 mL of Ni_A buffer with 80 mM imidazole), and eluted in a gradient elution from 80 mM imidazole to 1 M imidazole (50 mM Tris pH 8, 300 mM NaCl, 1 mM TCEP, 1 M imidazole) over 10 column volumes. Peak fractions were pooled, imidazole concentration lowered to less than 100 mM with Ni_A, and the sample was incubated with 0.01 mg/mL final TEV (made in-house) in order to cleave off the His₆ tag. On the following day, the cleaved protein was concentrated to 500 µL, using 50 kDa cut-off concentrator (4 mL Amicon R Ultra), and injected into Superose 6 10/300 column

(GE Healthcare) previously equilibrated in size exclusion (SEC) buffer (25 mM Tris pH 8, 250 mM NaCl, 1% glycerol, 1 mM TCEP). Elution profile of CaMKII^{L308BzF} comprised of three peaks: the first one which corresponded to Mw of dodecameric CaMKII (around 650 kDa), the second one which corresponded to ~40 kDa CaMKII fragment, which is usually present during CaMKII purification from *E. coli*, and the third one corresponding to ~35 kDa L308Stop fragment. The peak corresponding to dodecameric CaMKII was pooled and further concentrated to approximately 2 mg/mL. We obtained around 1–2 mg of protein per 2 L of *E. coli* culture.

The small-scale test purification reported in Figure 1b was performed using a modified version of the protocol described above. Upon clearance of cell lysate from 0.25 L of cell pellets, the lysate was then incubated with 1 mL of Co²⁺ beads. After 2 h incubation with the beads (rolling in a falcon tube at 4°C), the beads were spun down, the supernatant removed and beads resuspended in 15 mL of wash buffer (Ni_A buffer). After a few cycles of bead washing, the protein was cleaved from the beads, using TEV protease, overnight, rolling at 4°C. Cleaved protein was run on an SEC column, as described above.

4.5 | Calmodulin purification

Cell pellets from 4 L of bacterial cultures were lysed in 100 mL of lysis buffer (50 mM Tris pH 8, 150 mM NaCl, 1 mM PMSF, 0.02 mg/mL DNaseI, 5 mM MgCl₂, and 0.5 mg/mL lysozyme) for 1 h stirring at 4°C, followed by sonication on ice (6 × 25 s, 5 cycle, 50% power, 1 min pause between cycles). Cell lysates were cleared by centrifugation (16k rpm, 4°C for 30 min), and the supernatant was loaded on a 5 mL NiNTA column (GE Healthcare), previously equilibrated in Ni_A buffer (50 mM Tris pH 8, 150 mM NaCl, 5 mM MgCl₂ and 20 mM imidazole). His-tagged Calmodulin was eluted in a gradient elution, using Ni_B buffer (50 mM Tris pH 8, 150 mM NaCl, 5 mM MgCl₂, and 1 M imidazole). Peak fractions were pooled and incubated with 150 µL of 2 mg/mL TEV (made in-house) overnight. To optimize the cleavage conditions, imidazole concentration was lowered to under 100 mM, and 1 mM TCEP was added to the cleavage reaction. The purification was continued on the following day by loading the overnight sample onto a 1 mL Q column (GE Healthcare). To enable binding to the column, first, the salt concentration was lowered to about 40 mM NaCl by adding Q_A buffer (20 mM HEPES pH 7, 25 mM NaCl, 5 mM CaCl₂). Calmodulin was eluted from the column by gradient elution, using Q_B buffer (20 mM HEPES pH 7, 1 M NaCl, 5 mM CaCl₂).

Fractions were run on an SDS-PAGE gel to determine the peak fractions, because the 280 nm signal coming from Calmodulin is too low, as Calmodulin does not contain any Trp residues. The peak fractions were pooled and concentrated to 200 μ L. Calmodulin concentration was determined using Bradford assay and found to be around 0.8 mg/mL (47 μ M).

4.6 | UV-induced crosslinking

To drive crosslinking of CaMKII^{L308BzF} to Calmodulin, we used a UV LED that emits UV light of 365 nm wavelength (Opsytec Dr. Gröbel). Samples were placed in a cold metal plate (made in-house) in a cold room, to avoid damage caused by excess heating from the UV light. Each sample was illuminated 5 times using 15 1 s pulses of UV light, with a 1 s break in between each pulse. This was repeated 5 times per sample with a 1-min break between each series of pulses. Samples were in SEC buffer, supplemented with either 1 mM TCEP or 50 mM TCEP to avoid non-specific crosslinking due to oxidation of surface exposed Cysteines. The samples were then run on a 4%–12% gradient Bis-Tris gel (ThermoScientific), and stained with Coomassie dye (FastGene Q Stain from Nippongenetics).

4.7 | Determination of Calmodulin binding constant

CaMKII^{L308BzF} was incubated with His-tagged Calmodulin (Calbiochem, product # 208670-50UG). Final CaMKII^{L308BzF} concentration in 20 μ L of crosslinking reaction was set to 8 μ M in SEC buffer (50 mM Tris pH 8, 250 mM NaCl, 1% glycerol) supplemented with 50 mM TCEP. Final Calmodulin concentrations were 16, 8, 2.4, 1.2, 0.6, and 0.12 μ M, supplemented with 2 mM CaCl₂. Each crosslinking reaction was done in triplicate, using UV illumination protocol described in section 4.6. The samples were then run on a 4%–12% gradient Bis-Tris gel (ThermoScientific), and stained with Coomassie dye (FastGene Q Stain from Nippongenetics). Calmodulin binding constant was determined by measuring densitometry of monomeric CaMKII band depletion, using Fiji software. Densitometry determination on other bands was unsuccessful because the upper bands are more diffuse than the monomer band, which thanks to an exaggerated background contribution causes unrealistic increase in densitometry values of upper bands. Efforts to sum up the bands between lanes in order to compare them proved to be difficult, due to diffusive nature of the upper bands as well as the fact that different gels are and the staining on them are not identical. The K_d was

obtained by fitting the data points using IgorPro9 software. We fitted the data with a Langmuir function.

$$y = \frac{K_d}{K_d + [\text{CaM}]}$$

4.8 | Mass photometry

Mass photometry was performed on Refeyn One^{MP} mass photometer. Coverslips (Marienfeld high precision glass coverslips, 24 \times 50 mm #1.5H, 170 \pm 5 μ m; product # 0107222) were cleaned following the manufacturer's instructions. The coverslips were rinsed sequentially with purified miliQ H₂O, 100% EtOH, 100% isopropanol, miliQ H₂O, 100% EtOH, and miliQ H₂O several times, then dried under a clean stream of nitrogen.

The samples of CaMKII^{WT} were prepared by diluting 8 μ M CaMKII^{WT} with or without 2 μ M self-made Calmodulin, with or without UV exposure in buffer containing 25 mM Tris pH 8, 250 mM NaCl, 1% glycerol, 1 mM TCEP to obtain 1.6 μ M CaMKII^{WT}. The samples of CaMKII^{L308BzF} were prepared by diluting 8 μ M CaMKII^{L308BzF} with or without 8 μ M His-Calmodulin (Calbiochem), with or without UV exposure in buffer containing 25 mM Tris pH 8, 250 mM NaCl, 1% glycerol, 1 mM TCEP to obtain 1.6 μ M CaMKII^{WT}. Samples were initially incubated for 5 minutes at room temperature, before the first image acquisition. Each sequential measurement meant that the sample spent additional 1–2 min incubating before it could be recorded again, for each triplicate. Images were collected in an area of 3 \times 10 μ m, except for wild-type CaMKII in Figure 4a, c, e which were done with the large view (10 \times 10 μ m). CaMKII^{L308BzF} 8 μ M was also diluted to 0.4 μ M and 0.04 μ M. The recordings were made by diluting 5 μ L of stock samples (1.6, 0.4, or 0.04 μ M) in 15 μ L of buffer, directly on the cover slide. The final concentration of CaMKII (monomer concentration) in the drop was either 400 nM (for both CaMKII^{WT} or CaMKII^{L308BzF}), 100 nM or (CaMKII^{L308BzF}) 10 nM (CaMKII^{L308BzF}). The counts obtained for each measurement were fitted to a Gaussian fit using IgorPro9 software Multipeak fitting package.

4.9 | Kinase activity assay

The following master mixes were set up:

Master mix 1 (MM1) containing 4.4 μ M CaMKII^{WT}, 2.2 μ M self-made Calmodulin, 2.2 mM CaCl₂ in SEC buffer (with freshly added 50 mM TCEP), master mix 2 (MM2) containing 4 μ M Calmodulin, 4 mM CaCl₂, 14 mM EGTA (incubated for 5 min at 25°C to allow chelation of Ca²⁺), master mix 3 (MM3) containing 4 μ M

Calmodulin, 4 mM CaCl₂, 80 mM EGTA (incubated for 5 min at 25°C to allow chelation of Ca²⁺), master mix 4 (MM4) containing 4.4 μM CaMKII^{L308BzF}, 2.2 μM self-made Calmodulin, 2.2 mM CaCl₂ in SEC buffer (with freshly added 50 mM TCEP). Activation with ATP:Mg²⁺ was done at 37°C for 10 min, in all reactions where ATP:Mg²⁺ was added.

Reactions containing CaMKII^{WT} were set up, to obtain approximately final [CaMKII] = 4 μM, final [CaM] = 2 μM and [CaCl₂] = 2 mM, as follows:

Lane 1–9 μL of MM1 activated by adding 1 μL of 1 mM ATP/ 200 mM MgCl₂ to get final 100 μM ATP and 20 mM MgCl₂, lane 2–9 μL of MM1 with 1 μL of SEC buffer, lane 3–8 μL of MM1 incubated with 1 μL of 70 mM EGTA (final [EGTA] = 7 mM) for 5 min at 25°C, followed by activation by adding 1 μL of 1 mM ATP/ 200 mM MgCl₂ to get final 100 μM ATP: 20 mM MgCl₂, lane 4–8 μL of MM1 incubated with 1 μL of 400 mM EGTA for 5 min at 25°C (final [EGTA] = 40 mM, note, final CaMKII 3.5 μM in this reaction), followed by activation by adding 1 μL of 1 mM ATP/ 200 mM MgCl₂ to get final 100 μM ATP: 20 mM MgCl₂, lane 5–5 μL of MM2 with 4 μL of CaMKII^{WT} (9.9 μM) for 5 min at 25°C, then activated by adding 1 μL of 1 mM ATP/ 200 mM MgCl₂ to get final 100 μM ATP: 20 mM MgCl₂, lane 6–5 μL of MM3 with 4 μL of CaMKII^{WT} (9.9 μM) for 5 min at 25°C then activated by adding 1 μL of 1 mM ATP/ 200 mM MgCl₂ to get final 100 μM ATP: 20 mM MgCl₂.

Reactions containing CaMKII^{L308BzF} were set up, to obtain final [CaMKII] = 4 μM, final [CaM] = 2 μM and [CaCl₂] = 2 mM, as follows:

Lane 7–9 μL of MM4 activated by adding 1 μL of 1 mM ATP/ 200 mM MgCl₂ to get final 100 μM ATP and 20 mM MgCl₂, lane 8–9 μL of MM1 with 1 μL of SEC buffer, lane 9–9 μL of MM4 treated with UV and then activated by adding 1 μL of 1 mM ATP/ 200 mM MgCl₂ to get final 100 μM ATP and 20 mM MgCl₂, lane 10–8 μL of MM4 with 1 μL of 400 mM EGTA for 5 min at 25°C, followed by UV treatment and then addition of 1 μL of 1 mM ATP/ 200 mM MgCl₂ to get final 100 μM ATP and 20 mM MgCl₂ (note, final CaMKII 3.5 μM in this reaction and lanes 11 and 12).

Lane 11–8 μL of MM4 with 1 μL of 400 mM EGTA for 5 min at 25°C, without UV treatment, followed by the addition of 1 μL of 1 mM ATP/ 200 mM MgCl₂ to get final 100 μM ATP and 20 mM MgCl₂, lane 12–8 μL of MM4 was first treated with UV to obtain CaMKII:CaM crosslinks, then incubated with 1 μL of 400 mM EGTA for 5 min at 25°C, followed by activation with 1 μL of 1 mM ATP/ 200 mM MgCl₂ to get final 100 μM ATP and 20 mM MgCl₂, lane 13–5 μL of MM2 with 4 μL of CaMKII^{L308BzF} (9.9 μM) for 5 min at 25°C, then activated by adding 1 μL of 1 mM ATP/ 200 mM MgCl₂ to get final 100 μM ATP: 20 mM MgCl₂, and then treated with UV,

lane 14–5 μL of MM3 with 4 μL of CaMKII^{L308BzF} (9.9 μM) for 5 min at 25°C, then activated by adding 1 μL of 1 mM ATP/ 200 mM MgCl₂ to get final 100 μM ATP: 20 mM MgCl₂, and then treated with UV.

The kinase assays were repeated with newly purified CaMKII^{WT} and CaMKII^{L308BzF}, using His-Calmodulin from Calbiochem. The master mixes were set up like before, but this time using equimolar amounts of CaMKII and His-Calmodulin. The following master mixes were set up: master mix 1 (MM1) containing 4.4 μM CaMKII^{WT}, 4.4 μM His-Calmodulin, 2.2 mM CaCl₂ in SEC buffer (with freshly added 50 mM TCEP), master mix 2 (MM2) containing 8 μM His-Calmodulin, 4 mM CaCl₂, 14 mM EGTA (incubated for 5 min at 25°C to allow chelation of Ca²⁺), master mix 3 (MM3) containing 8 μM Calmodulin, 4 mM CaCl₂, 80 mM EGTA (incubated for 5 min at 25°C to allow chelation of Ca²⁺), master mix 4 (MM4) containing 4.4 μM CaMKII^{L308BzF}, 4.4 μM self-made Calmodulin, 2.2 mM CaCl₂ in SEC buffer (with freshly added 50 mM TCEP). The reactions were set up like those described above. Conditions in each lane are described in Figure S3 legend. Controls for basal CaMKII activity (no Calmodulin) were added (lanes 7 and 8).

4.10 | Kinase activity assay with peptide-substrate

Peptide-substrate (Syntide from GenScript) phosphorylation was measured using ADPQuest according to the manufacturer instructions. Reactions were set up in a 96-well plate and the kinase reaction was monitored using a TECAN plate reader. Briefly, activity of 100 nM CaMKII toward 50 μM Syntide, incubated with 100 μM ATP/200 μM MgCl₂ and 1.5 μM Ca²⁺:Calmodulin, was measured for 40 min, at 37°C. Recordings were made every 5 min.

4.11 | Western blot detection on samples from in vitro kinase assays

First, 500 ng of CaMKII protein was loaded per lane of a pre-casted 4%–12% gradient BisTris gel (ThermoScientific) to allow protein separation, followed by transfer to pre-activated (in 100% MeOH) PVDF membrane (Millipore) for 2 h at 50 V at 8°C, using Criterion Blotter (BioRad) in Twobin's transfer buffer with 20% MeOH. Membranes were then blocked in Tris Buffer Saline (TBS) with 0.1% Tween and 5% Milk (Sigma Aldrich) for 1 h shaking at room temperature. The membranes were incubated with two primary antibodies at the same time (mouse anti-human pan CaMKII G69 from CellSignaling (product

#50049S), and rabbit anti-pT286 from CellSignaling (product #12716S)), in 5% milk/TBS-T over-night at 4°C. On the following day, the membranes were washed 3× in TBS-T and incubated with secondary antibodies (fluorescently labeled IRDye 800CW Goat-anti Rabbit IgG and IRDye 680LT Goat-anti Mouse IgG from LiCor) for 1 h shaking at room temperature, followed by 3× washing in TBS-T. This allowed simultaneous detection of both total CaMKII (excited with 700 nm wavelength) and phosphorylation at T286 (excited with 800 nm wavelength) signals, using a LiCor imager.

4.12 | HEK cell transfection and lysis

HEK 293 cells (ACC-305) were purchased from Leibniz Institute DSMZ (German Collection of Microorganisms and Cell Cultures GmbH, Braunschweig). In-house testing for mycoplasma yielded a negative result.

A total of 1 million cells were seeded per one well of a 6-well dish. The cells were transfected on the following day using polyethylenimine (PEI), in a DNA:PEI ratio of 1:3. Total of 3 µg of DNA with CaMKII^{L308TAG}:tRNA:RS ratio of 4:1:1 (2 µg of CaMKII^{L308TAG}, 0.5 µg of tRNA and 0.5 µg of RS) was mixed with 9 µL of PEI in 250 µL pre-warmed optiMEM. After 4–5 h the media was changed to remove the transfection reagent and to add fresh media supplemented with BzF (1, 5, or 10 mM). Cells were harvested after 24–48 h, by adding 1 mL of ice-cold DPBS per well, and centrifugation at 2000 rpm for 5 min in a cooled table-top centrifuge. The cell pellets were then lysed in 100 µL of ice cold lysis buffer (50 mM Tris pH 8, 150 mM NaCl, 1% Triton X 100, 1 mM TCEP, 1 µM Pepstatin A, 10 µM Leupeptin, 0.3 µM Aprotinin, 1 mM PMSF, 5 mM NaF, 0.02 mg/mL DNaseI and 5 mM MgSO₄) on ice, for 20 min, with vortexing every 5 min. The lysates were then cleared by high-speed centrifugation for 15 min in a cooled tabletop centrifuge. Supernatants, containing CaMKII were subjected to Western Blot analysis.

4.13 | Western blot detection on HEK cell lysates

A total of 21 µL of each lysate was combined with 7 µL of 4 × SDS loading dye and incubated at 95°C for 2 minutes to aid protein denaturation. A total of 20 µL of each sample was loaded on 4%–12% pre-casted gel (Thermo Scientific), and ran for 1 h 20 min at 180 V in cold 1 × MOPS buffer. The transfer to the PVDF membrane and the rest of the western blotting protocol was the same as in Section 4.11.

4.14 | Intact mass spectrometry

Measurements were performed on the AB SCIEX 5800 TOF/TOF system (Applied Biosystems, California, USA). The protein concentration used was 0.8 mg/mL. A total of 1 µL of this sample was then mixed with 1 µL of a matrix solution of 5 mg/mL α -cyano-4-hydroxycinnamic acid in acetonitrile/water (1:1, v:v), 0.3% TFA on the sample plate. The sample was air dried for 10 min at room temperature. The measurements took place in positive linear mode (measuring range 20,000–100,000 Da). The graphical analysis of the spectra was performed using Data Explorer[®] software version 4.1 (Applied Biosystems, California, USA).

4.15 | Preparation of samples for mass spectrometry

Four replicates of the following samples were run on a 12% home-made SDS denaturing gel for 1 h 20 min on 180 V: CaMKII^{L308BzF} treated with UV, untreated CaMKII^{L308BzF}, CaMKII^{L308BzF} incubated with Ca²⁺:Calmodulin and then treated with UV, untreated CaMKII^{L308BzF} incubated with Ca²⁺:Calmodulin. Both Calmodulin and CaMKII^{L308BzF} concentrations were set to 8 µM and Ca²⁺ to 2 mM in CaMKII size exclusion buffer (25 mM Tris pH 8.0, 250 mM NaCl, 1% Glycerol) supplemented with 1 mM TCEP. After electrophoresis, the gels were stained with Coomassie dye, and rinsed with water, and CaMKII^{L308BzF} bands were excised using a clean scalpel. Gel slices were then subjected to in-gel digestion.

4.16 | In-gel digestion of mass spec samples

Excised gel slices were preserved in 50 mM Triethylammonium bicarbonate buffer (TEAB, Sigma-Aldrich). The gel sections were fragmented into smaller pieces and subjected to sequential washing with 50% Acetonitrile (ACN, Fisher Chemical) and 100% ACN buffers. Following alkylation with 50 mM chloroacetamide (CAA, Sigma-Aldrich), the gel pieces underwent an overnight digestion with a 1:40 (w/w) ratio of Lysyl endopeptidase C (FUJIFILM Wako Chemicals) and a 1:20 (w/w) ratio of Trypsin (Serva). The digestion buffer including tryptic peptides was subsequently transferred to new tubes. Gel pieces were then washed twice with 50% ACN to complete the peptide extraction process and transferred to new tubes. Collected samples were subsequently desiccated.

4.17 | LC-MS/MS analysis

The desiccated samples were re-suspended with 20 μ L of 0.1% Formic Acid (FA, Biosolve Chimie SARL). The LC-MS/MS analysis was performed on the UHPLC Vanquish Neo cooperated with Orbitrap Exploris 480 from Thermo Fisher Scientific. For each sample, 0.25 μ L was loaded and fractionated on a 50 cm analytical column (in-house packed with Poroshell 120 EC-C₁₈, 1.7 μ m, Agilent Technologies) with reverse-phase gradient. The mobile phase buffer A was composed of 0.1% Formic Acid in ddH₂O and mobile phase buffer B was composed of 0.1% Formic Acid in 80% Acetonitrile (FA, Biosolve Chimie SARL). The gradient started at 4% buffer B then linearly increased to 22.5% in 50 min, followed by a linear increase to 45% buffer B in the following 17 min. During the next 0.5 min, the mobile phase was raised to 99% buffer B and washed for another 12 min. The flow was pumped with 0.25 μ L/min.

Analytes were sprayed with nano-electrospray ion source and then guided into Orbitrap Exploris 480. Samples were analyzed under data-dependent mode with positive charge +2 to +4. The orbitrap resolution was set to 120,000 with a scan range (m/z) 375–1200 and 300% normalized automatic gain control target. The peptide dissociation was executed with HCD collision energy 30% with resolution 15,000, isolation window (m/z) 1.6. Ions were selected with criteria 1.0e4 intensity threshold coupled with 20 s exclusion duration.

4.18 | Mass spec data analysis

The acquired raw data were subjected to analysis using MaxQuant 2.4.2.0, searching against the CaMKII^{L308BzF} and Calmodulin sequences for the database. The following modifications were considered as variable modifications: Oxidation (M), Acetylation (N-terminus), and Carbamidomethylation (C). These modifications were considered as variable modifications for the analysis. FTMS MS/MS tolerance was set to 20 ppm. Both PSM FDR and Protein FDR were set to 0.01. The ratio-modified: base was used for ANOVA and Student *t*-test analysis.

AUTHOR CONTRIBUTIONS

Iva Lučić: Conceptualization (equal); data curation (equal); formal analysis (equal); funding acquisition (supporting); investigation (equal); methodology (equal); project administration (equal); validation (equal); visualization (equal); writing – original draft (equal); writing – review and editing (equal). **Pin-Lian Jiang:** Investigation (supporting); visualization (equal); writing – review and editing (supporting).

Andreas Franz: Conceptualization (supporting); investigation (supporting); methodology (supporting); writing – review and editing (supporting). **Yuval Bursztyn:** Investigation (supporting). **Fan Liu:** Formal analysis (supporting); investigation (supporting); supervision (equal). **Andrew J. R. Plested:** Conceptualization (equal); data curation (equal); formal analysis (equal); funding acquisition (equal); methodology (equal); project administration (equal); resources (equal); supervision (equal); validation (equal); visualization (equal); writing – original draft (equal); writing – review and editing (equal).

ACKNOWLEDGMENTS

We are grateful to Alejandro Castro Scalise for purifying Calmodulin, Heike Nikolenko (FMP-Berlin) for intact mass determinations, and Jörg Malsam (BzH, Heidelberg, Germany) for the assistance with expression of BzF-containing proteins in *E. coli*. Iva Lučić was recipient of a Marie Curie Incoming International Fellowship (798696) and “Wiedereinstiegsstipendium” from the Leibniz FMP. This work was funded by the DFG TRR 186 (Project A07, *Projektnummer* 278001972 to Andrew J. R. Plested), a DFG Heisenberg Professorship (to Andrew J. R. Plested, *Projektnummern* 323514590 & 446182550), and the European Research Council (ERC-STG no. 949184 to Fan Liu). Andreas Franz was recipient of a Boehringer Ingelheim PhD Fellowship. Molecular graphics and analyses performed with UCSF ChimeraX, developed by the Resource for Biocomputing, Visualization, and Informatics at the University of California, San Francisco, with support from National Institutes of Health R01-GM129325 and the Office of Cyber Infrastructure and Computational Biology, National Institute of Allergy and Infectious Diseases.

CONFLICT OF INTEREST STATEMENT

The authors declare no conflicts of interest.

DATA AVAILABILITY STATEMENT

All relevant data are provided in the paper.

ORCID

Andrew J. R. Plested  <https://orcid.org/0000-0001-6062-0832>

REFERENCES

- Albanese SK, Parton DL, Işık M, L Rodríguez-Laureano, SM Hanson, JM Behr, et al. An open library of human kinase domain constructs for automated bacterial expression. *Biochemistry*. 2018;57(31):4675–89. <https://doi.org/10.1021/acs.biochem.7b01081>
- Bear MF, Cooke SF, Giese KP, Kaang BK, Kennedy MB, Kim JL, et al. In memoriam: John Lisman—commentaries on CaMKII

- as a memory molecule. *Mol Brain*. 2018;11(1):76. <https://doi.org/10.1186/s13041-018-0419-y>
- Bhattacharyya M, Stratton MM, Going CC, McSpadden ED, Huang Y, Susa AC, et al. Molecular mechanism of activation-triggered subunit exchange in Ca²⁺/calmodulin-dependent protein kinase II. *Elife*. 2016;5:1–32. <https://doi.org/10.7554/eLife.13405>
- Bindels DS, Haarbosch L, van Weeren L, Postma M, Wiese KE, Mastop M, et al. MScarlet: a bright monomeric red fluorescent protein for cellular imaging. *Nat Methods*. 2017;14(1):53–6. <https://doi.org/10.1038/nmeth.4074>
- Chang JY, Parra-Bueno P, Laviv T, Szatmari EM, Lee SJR, Yasuda R. CaMKII autophosphorylation is necessary for optimal integration of Ca²⁺ signals during LTP induction, but not maintenance. *Neuron*. 2017;94(4):800–808.e4. <https://doi.org/10.1016/j.neuron.2017.04.041>
- Chao LH, Pellicena P, Deindl S, Barclay LA, Schulman H, Kuriyan J. Intersubunit capture of regulatory segments is a component of cooperative CaMKII activation. *Nat Struct Mol Biol*. 2010;17(3):264–72. <https://doi.org/10.1038/nsmb.1751>
- Chao LH, Stratton MM, Lee IH, Rosenberg OS, Levitz J, Mandell DJ, et al. A mechanism for tunable autoinhibition in the structure of a human Ca²⁺/calmodulin-dependent kinase II holoenzyme. *Cell*. 2011;146(5):732–45. <https://doi.org/10.1016/j.cell.2011.07.038>
- Chen X, Cai Q, Zhou J, Pleasure SJ, Schulman H, Zhang M, et al. CaMKII autophosphorylation but not downstream kinase activity is required for synaptic memory. *bioRxiv [Preprint]* 2023; (415):1–21 <https://doi.org/10.1101/2023.08.25.554912>
- Chin D, Means AR. Calmodulin: a prototypical calcium sensor. *Trends Cell Biol*. 2000;10(8):322–8.
- Colgan LA, Hu M, Mislser JA, Parra-Bueno P, Moran CM, Leitges M, et al. PKC α integrates spatiotemporally distinct Ca²⁺ and autocrine BDNF signaling to facilitate synaptic plasticity. *Nat Neurosci*. 2018;21:1027–37. <https://doi.org/10.1038/s41593-018-0184-3>
- Crick F. Memory and molecular turnover. *Nature*. 1984;312(5990):101. <https://doi.org/10.1038/312101a0>
- Giron P, Dayon L, Sanchez JC. Cysteine tagging for MS-based proteomics. *Mass Spectrom Rev*. 2011;30(3):366–95. <https://doi.org/10.1002/mas.20285>
- Goodman JK, Zampronio CG, Jones AME, Hernandez-Fernaund JR. Updates of the in-gel digestion method for protein analysis by mass spectrometry. *Proteomics*. 2018;18(23):1–5. <https://doi.org/10.1002/pmic.201800236>
- Herring BE, Nicoll RA. Long-term potentiation: from CaMKII to AMPA receptor trafficking. *Annu Rev Physiol*. 2016;78:351–65. <https://doi.org/10.1146/annurev-physiol-021014-071753>
- Hoffman L, Stein RA, Colbran RJ, McHaourab HS. Conformational changes underlying calcium/calmodulin-dependent protein kinase II activation. *Embo J*. 2011;30(7):1251–62. <https://doi.org/10.1038/emboj.2011.40>
- Incontro S, Díaz-Alonso J, Iafrazi J, Vieira M, Asensio CS, Sohal VS, et al. The CaMKII/NMDA receptor complex controls hippocampal synaptic transmission by kinase-dependent and independent mechanisms. *Nat Commun*. 2018;9(1):1–21. <https://doi.org/10.1038/s41467-018-04439-7>
- Johannessen CM, Boehm JS, Kim SSS, Thomas SR, Wardwell L, Johnson LA, et al. COT expression predicts resistance to B-RAF inhibition in cancer cell lines. *Nature*. 2011;468(7326):968–72. <https://doi.org/10.1038/nature09627>
- Jurado LA, Chockalingam PS, Jarrett HW. Apocalmodulin. *Physiol Rev*. 2022;79(3):661–82.
- Karandur D, Bhattacharyya M, Xia B, Lee YK, Muratcioglu S, McAfee D, et al. Breakage of the oligomeric CaMKII hub by the regulatory segment of the kinase. *bioRxiv* 2020:1–31 <https://doi.org/10.1101/2020.04.15.043067>
- Kim K, Saneyoshi T, Hosokawa T, Okamoto K, Hayashi Y. Interplay of enzymatic and structural functions of CaMKII in long-term potentiation. *J Neurochem*. 2016;139(6):959–72. <https://doi.org/10.1111/jnc.13672>
- Klán P, Šolomek T, Bochet CG, Blanc A, Givens R, Rubina M, et al. Photoremovable protecting groups in chemistry and biology: reaction mechanisms and efficacy. *Chem Rev*. 2013;113(1):119–91. <https://doi.org/10.1021/cr300177k>
- Klippenstein V, Ghisi V, Wietstruk M, Pleded AJR. Photoinactivation of glutamate receptors by genetically encoded unnatural amino acids. *J Neurosci*. 2014;34(3):980–91. <https://doi.org/10.1523/JNEUROSCI.3725-13.2014>
- Lee J, Chen X, Nicoll RA. Synaptic memory survives molecular turnover. *Proc Natl Acad Sci USA*. 2022;119(42):1–5. <https://doi.org/10.1073/pnas.2211572119>
- Lisman J, Schulman H, Cline H. The molecular basis of CaMKII function in synaptic and behavioural memory. *Nat Rev Neurosci*. 2002;3(3):175–90. <https://doi.org/10.1038/nrn753>
- Lučić I, Héluin L, Jiang PL, Castro Scalise AG, Wang C, Franz A, et al. CaMKII autophosphorylation can occur between holoenzymes without subunit exchange. *Elife*. 2023;12:1–29. <https://doi.org/10.7554/eLife.86090>
- Myers JB, Zaegel V, Coultrap SJ, Miller AP, Bayer KU, Reichow SL. The CaMKII holoenzyme structure in activation-competent conformations. *Nat Commun*. 2017;8:1–14. <https://doi.org/10.1038/ncomms15742>
- Nicoll RA. A brief history of long-term potentiation. *Neuron*. 2017;93(2):281–90. <https://doi.org/10.1016/j.neuron.2016.12.015>
- Nikić-Spiegel I. Expanding the genetic code for neuronal studies. *Chembiochem*. 2020;21(22):3169–79. <https://doi.org/10.1002/cbic.202000300>
- Okamoto K, Narayanan R, Lee SH, Murata K, Hayashi Y. The role of CaMKII as an F-actin-bundling protein crucial for maintenance of dendritic spine structure. *Proc Natl Acad Sci USA*. 2007;104(15):6418–23. <https://doi.org/10.1073/pnas.0701656104>
- Otmakhov N, Lisman J. Measuring CaMKII concentration in dendritic spines. *J Neurosci Methods*. 2012;203(1):106–14. <https://doi.org/10.1016/j.jneumeth.2011.09.022>
- Murakoshi H, Shin ME, Parra-Bueno P, Szatmari EM, Shibata ACE, Yasuda R. Kinetics of endogenous CaMKII required for synaptic plasticity revealed by optogenetic kinase NeuroResource kinetics of endogenous CaMKII required for synaptic plasticity revealed by optogenetic kinase inhibitor. *Neuron*. 2017;94(1):37–47.e5. <https://doi.org/10.1016/j.neuron.2017.02.036>
- Poulsen MH, Poshtiban A, Klippenstein V, Ghisi V, Pleded AJR. Gating modules of the AMPA receptor pore domain revealed by unnatural amino acid mutagenesis. *Proc Natl Acad Sci USA*. 2019;116(27):13358–67. <https://doi.org/10.1073/pnas.1818845116>
- Rellos P, Pike ACW, Niesen FH, Salah E, Lee WH, von Delft F, et al. Structure of the CaMKII δ /calmodulin complex reveals the

- molecular mechanism of CamKII kinase activation. *PLoS Biol.* 2010;8(7):e1000426. <https://doi.org/10.1371/journal.pbio.1000426>
- Rocco-Machado N, Lai L, Kim G, He Y, Luczak ED, Anderson ME, et al. Oxidative stress—induced autonomous activation of the calcium/calmodulin-dependent kinase II involves disulfide formation in the regulatory domain. *J Biol Chem.* 2022;298:28–31. <https://doi.org/10.1016/j.jbc.2022.102579>
- Rossetti T, Banerjee S, Kim C, Leubner M, Lamar C, Gupta P, et al. Memory erasure experiments indicate a critical role of CaMKII in memory storage. *Neuron.* 2017;96(1):207–216.e2. <https://doi.org/10.1016/j.neuron.2017.09.010>
- Shibata ACE, Ueda HH, Eto K, Onda M, Sato A, Ohba T, et al. Photoactivatable CaMKII induces synaptic plasticity in single synapses. *Nat Commun.* 2021;12(1):1–15. <https://doi.org/10.1038/s41467-021-21025-6>
- Shifman JM, Choi MH, Mihalas S, Mayo SL, Kennedy MB. Ca²⁺/calmodulin-dependent protein kinase II (CaMKII) is activated by calmodulin with two bound calciums. *Proc Natl Acad Sci USA.* 2006;103(38):13968–73. <https://doi.org/10.1073/pnas.0606433103>
- Stratton M, Lee IH, Bhattacharyya M, Christensen SM, Chao LH, Schulman H, et al. Activation-triggered subunit exchange between CaMKII holoenzymes facilitates the spread of kinase activity. *Elife.* 2014;3:e01610. <https://doi.org/10.7554/eLife.01610>
- Takemoto-Kimura S, Suzuki K, Horigane SI, Kamijo S, Inoue M, Sakamoto M, et al. Calmodulin kinases: essential regulators in health and disease. *J Neurochem.* 2017;141(6):808–18. <https://doi.org/10.1111/jnc.14020>
- Tao W, Lee J, Chen X, Diaz-Alonso J, Zhou J, Pleasure S, et al. Synaptic memory requires CaMKII. *Elife.* 2021;10:1–20. <https://doi.org/10.7554/eLife.60360>
- Torres-Ocampo AP, Özden C, Hommer A, Gardella A, Lapinskas E, Samkutty A, et al. Characterization of CaMKII α holoenzyme stability. *Protein Sci.* 2020;29(6):1524–34. <https://doi.org/10.1002/pro.3869>
- Tullis JE, Larsen ME, Rumian NL, Freund RK, Boxer EE, Brown CN, et al. LTP induction by structural rather than enzymatic functions of CaMKII. *Nature.* 2023;621(October 2022):146–53. <https://doi.org/10.1038/s41586-023-06465-y>
- Ye S, Köhrer C, Huber T, Kazmi M, Sachdev P, Yan ECY, et al. Site-specific incorporation of keto amino acids into functional G protein-coupled receptors using unnatural amino acid mutagenesis. *J Biol Chem.* 2008;283(3):1525–33. <https://doi.org/10.1074/jbc.M707355200>
- Young G, Hundt N, Cole D, Fineberg A, Andrecka J, Tyler A, et al. Quantitative mass imaging of single molecules HHS public access. *Science.* 2018;360(6387):423–7. <https://doi.org/10.1126/science.aar5839>
- Young TS, Ahmad I, Yin JA, Schultz PG. An enhanced system for unnatural amino acid mutagenesis in *E. coli*. *J Mol Biol.* 2010;395(2):361–74. <https://doi.org/10.1016/j.jmb.2009.10.030>

SUPPORTING INFORMATION

Additional supporting information can be found online in the Supporting Information section at the end of this article.

How to cite this article: Lučić I, Jiang P-L, Franz A, Bursztyn Y, Liu F, Plested AJR. Controlling the interaction between CaMKII and Calmodulin with a photocrosslinking unnatural amino acid. *Protein Science.* 2023;32(11):e4798. <https://doi.org/10.1002/pro.4798>